Available online www.jocpr.com

Journal of Chemical and Pharmaceutical Research, 2014, 6(6):1572-1578

Research Article

ISSN : 0975-7384
CODEN(USA) : JCPRC5

Numerical simulation and optimization design of a two-stage Laval annular mechanical foam breaker

Wang Jin-song, Cao Pin-lu* and Yin Kun

College of Construction Engineering, Jilin University, Changchun, China

---

ABSTRACT

A novel two-stage Laval annular mechanical foam breaker was designed which primarily uses the vacuum generated by the Coanda effect and the Laval principle to break foam. The value and the distribution of the negative pressure inside the foam breaker are very important to its performance. Here, we employ the computational fluid dynamics (CFD) code FLUENT to simulate the flow characteristics inside the foam breaker. The simulation results showed that the maximum velocity and negative pressure which generated in nearby the second throat plane is about 520m/s and -62kpa,respectively. The range of the internal negative pressure is larger than that of the others when the angle of the first diffuser is 0 and the annular slit distance is 150 mm.

Keywords: annular foam breaker, laval nozzle, CFD analysis, foam drilling

---

INTRODUCTION

As a new underbalanced drilling technology, foam drilling is often used for exploring low pressure and low permeability reservoirs (Wan et al., 2010; Zhao 1999).However, the main challenge of this technology is that the foam remains stable and requires a long period to dissipate back into the volume of the original liquid after emerging to the surface as a result of the long half-life and high stability of the foam fluid (Teichrob and Manuel, 1997; Chen 2005; Cao et al., 2009). Thus, foam drilling fluid can only be used once; an enormous volume of prepared foam liquid is required and an abundance of water and ingredient additives are consumed, which greatly increases the cost of foam drilling (Song et al., 1998; Paknejad 2005; Liu et al.2006).

The most widely used and high-efficiency method used at present is chemical defoaming that uses additives for foam breaking (Nethling et al., 2003; Wang et al., 2011). However, all chemical additives easily pollute the foaming surfactant and reduce its foamability. Thus, the foam base fluid cannot be used or the additives have a negative effect on the environment (Pelton 2002). In addition, the foam drilling fluid requires a large number of additives, which greatly increases drilling cost. However, the efficiency of most mechanical foam breakers, such as high rotate centrifugal foam breakers (Vetoshkin 2003), foam-breaking cyclones (Guzman 2005), and air jet breaker (Vetoshkin and Chagin 2002; Deshpande and Barigou 2000; Satoshi et al., 2003; Takesono et al., 2006; Zagoskina and Sokovnin 2001; Barigou 2001; Satoshi et al. 2007) is so low that they are hardly practical if the foam is excessive or the liquid phase viscosity is too high.

Annular foam breakers combine the two effects of vacuum and shear force to break foam, a process that achieved effective results during experimentation and application in the field of oil and gas well drilling and geological core drilling (Cao et al. 2011; Cao et al. 2012a,2012b; Hazaea et al. 2007). However, certain bubbles may not have sufficient time to burst because of the narrow range of negative pressure. Moreover, sometimes these breakers are do not effectively break foam on the condition that the foam velocity is too fast or the liquid phase viscosity is excessively high.

In this paper, the two-stage Laval annular mechanical foam breakers with different structures were designed. The flow characteristics inside the annular foam breaker were simulated numerically using the computation fluid dynamics software FLUENT to optimize the structure of the annular foam breaker.

1. The two-stage Laval annular mechanical foam breaker

The scheme of the two-stage annular mechanical foam breaker is shown in Fig. 1. Compressed gas enters the circular cavity from the air channel, passes through the Laval nozzle at supersonic speed, and then a negative pressure zone is generated near the throat after adhering to the convergent slot walls. When the foam drilling fluid flows through this negative pressure region, it bursts under the effect of the pressure difference. Moreover, considering the compressible mixing effects, the high-speed airflow interacts with the relatively low-speed foam fluid in the jet body chamber, and then mixes all along the length of the jet body and the diffuser. The difference in velocity between the air-stream and the foam drilling fluid transfers the momentum from the high velocity air to the foam fluid, which creates a powerful shear force that collapses the bubbles.

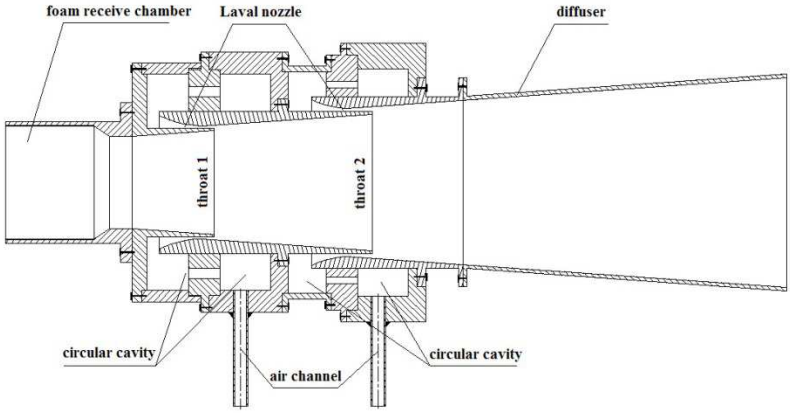

Figure 1.The two-stage Laval annular mechanical foam breaker

The two-stage Laval annular mechanical foam breaker primarily uses the vacuum effect to break the foam. Thus, the flow-field inside the annular foam breaker greatly affects its defoaming efficiency.

2. Flow characteristic of the foam breaker

3.1 Analytical model

The analytical model of the two-stage Laval annular foam breaker is shown in Fig. 2. Keeping the shape and size of the nozzle unchanged, the second nozzle is designed behind the first. Similar to the single annular foam breaker, many parameters can affect its performance, including the geometrical parameters of the Coanda surface, the length and the angle of the diffuser, and the size of the Laval nozzle. Here, we use the structural parameters from the document as follows: D1=80 mm, D2=D3=60 mm, D4=160 mm, R=100 mm, L1=550 mm, L2=70 mm, L3=400 mm, d=50 mm, θ=8°. Where D1 and D4 are the diameters of the foam entrance plane and the exit plane of the diffuser, respectively; D2 and D3 are the diameters of the throat plane of the foam breaker; L3 is the length of the diffuser; R is the radius of the Coanda surface; d is the annular slit distance; and θ is the diffuser angle.

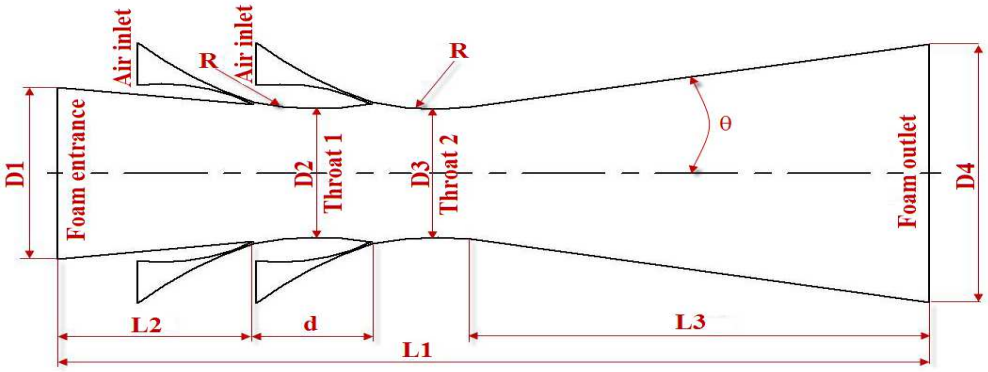

Figure.2.The analytical model of the two-stage Laval annular foam breaker

3.2 Basic assumptions and boundary conditions

Figure 3 illustrates the boundary conditions for numerical analysis. The foam breaker can be simplified to become two-dimensional axisymmetrical based on its structure characteristics. The dense meshes are preset at the areas that exhibit high flow rates and high-pressure gradients to obtain accurate results. The mass flow inlet and the pressure inlet are applied to the boundaries of the air channel and the foam channel, respectively. The initial mass flow rate is about 0.10 kgs^{-1} for both air inlets. Given that the foam burst process is very complicated and difficult to simulate, the pressure inlet boundary is set to atmospheric conditions to simplify the calculation. The couple implicit method was used in this calculation. The realizable *k-ε* turbulence model is selected whereas the standard near wall function is used in the near wall treatment. The near wall treatment becomes the standard wall function, which gives reasonably accurate results for the wall bounded with a very high Reynolds number flow.

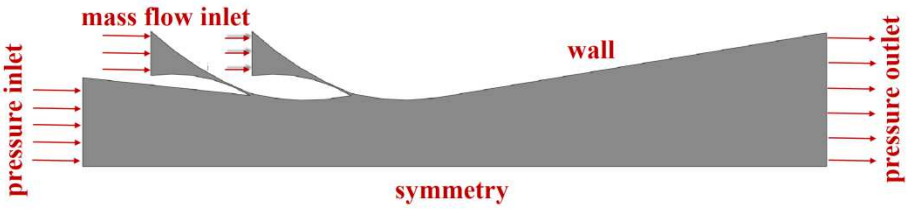

Figure.3. The boundary conditions of model

RESULTS AND DISCUSSION

The velocity and pressure distribution inside the two-stage Laval annular foam breaker are provided in Figs. 4 and 5, respectively. The velocity distribution contour shows that the high speed air coming from the first Laval annular slit adheres to the arc surface owing to the Coanda effect and then arrives at the arc surface of the second annular slit. Here, they meet with another high-speed flow that is ejected from the second annular slit and continues to move forward as a whole along the diffuser. Its maximum velocity is approximately 520 ms^{-1}, which was derived from around the second throat plane, as shown in Fig. 4(b). Figure 5 shows that negative pressure is generated near each Coanda surface and the maximum negative pressure is approximately 62kpa, which was generated near the second throat plane.

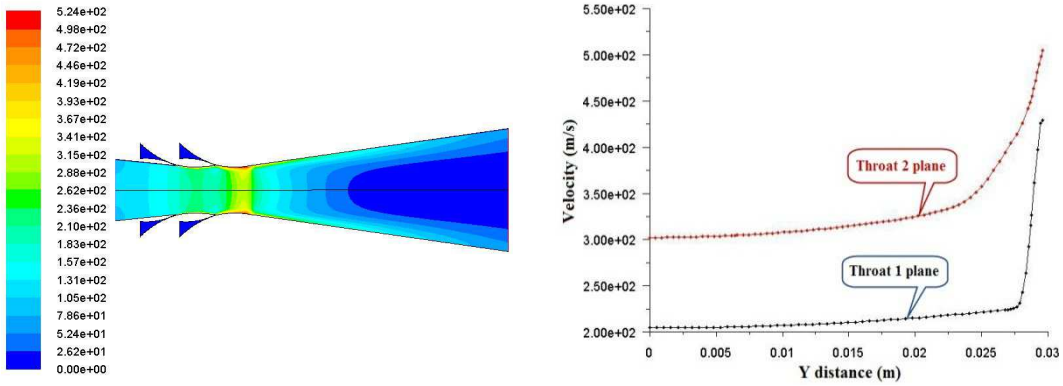

(a) Velocity distribution contours **(b) Velocity distribution of throat plane**

Figure.4. Velocity distribution inside the foam breaker (ms-1)

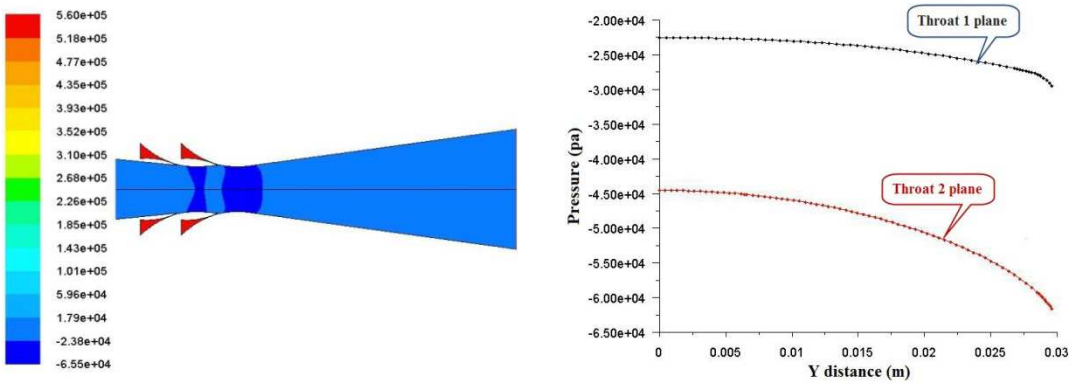

(b) Static pressure contours **(b) static pressure of throat plane**

Figure.5. Static pressure distribution inside the foam breaker (pa)

Compared with the single common annular foam breaker, the two-stage Laval annular foam breaker adds another Laval nozzle behind the first one, as illustrated in Fig.1. The distance between the two annular slits greatly affects the internal pressure distribution of the foam breaker. We designed three different of the two-stage Laval annular foam breaker model structures and simulated the inner flow-field to acquire the proper annular slit distance.

3. Optimization of annular slit distance

The first type of two-stage Laval annular foam breaker is designed based on the above analysis. This type of breaker retains the other structural parameters and the angles of both diffusers are 8°(θ´=θ=8°). Only the total length L1 and the second throat plane D3 are changed when the distances of two annular slits differ. The analytical model of the foam breaker is shown in Fig. 6. Considering the overall size and weight factors of the foam breaker, the distance between the two annular slits varied from 50 mm to 150 mm.

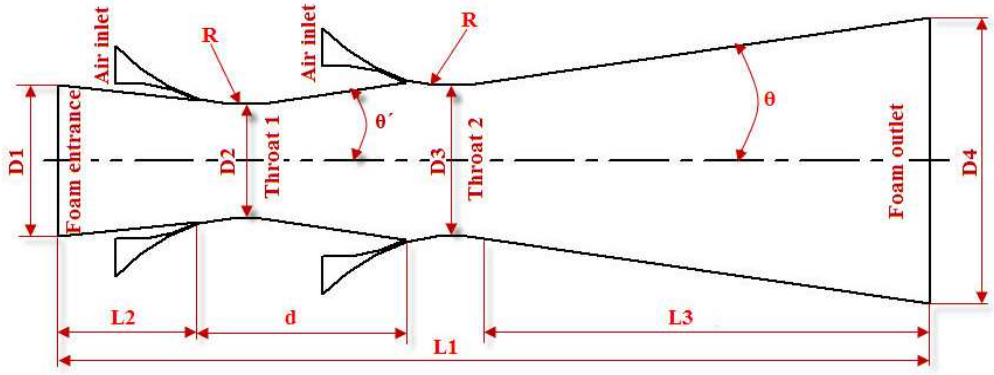

Figure.6. Analytical model of the first kind of foam breaker

Figure 7 shows that the value of the pressure near the first slit is approximately -30 kPa, whereas it is about -42 kPa near the second slit when the distance of the annular slits is 50 mm. When the distance increases to 70 mm, the value of the first pressure valley is approximately -45kPa, and that of the second is approximately -22 kPa. Thereafter, as annular slit distance increases, the value of both pressure valleys decreases and the second stage pressure valley decreases greatly. When the distance of the annular slit increases to 150 mm, the second stage pressure valley somewhat disappears. Thus, the best distance is 50 mm.

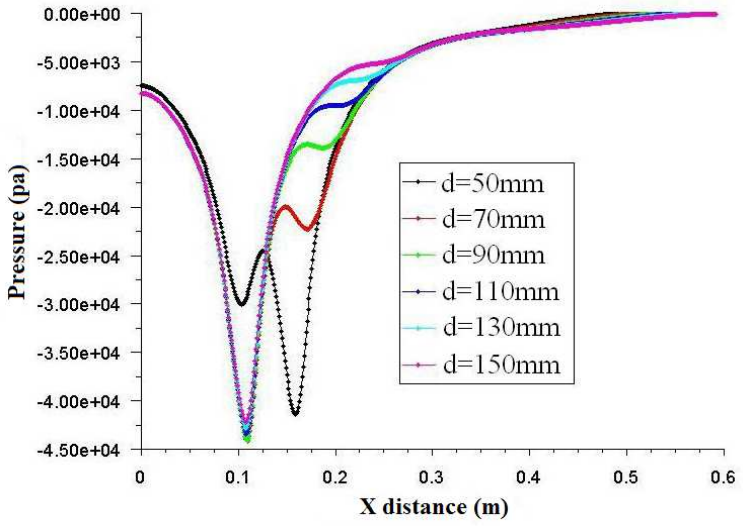

Figure.7. The pressure distribution along the center axis of the foam breaker(y=0)

Figure 7 also shows that the pressure distribution curve along the center axis differs from the others when the annular slit distance d=50 mm. This result is mainly because both throat plane dimensions are basically the same when the annular slit distance is 50 mm.

The above analysis of numerical simulation shows that the second throat dimension is important to the distribution of the inner flow-field of the two-stage foam breaker. Thus, we established the second geometric analytical model for further studies in Fig. 8. This model keeps both throat planes equal (D2=D3=60 mm) and only changes the total length L1.

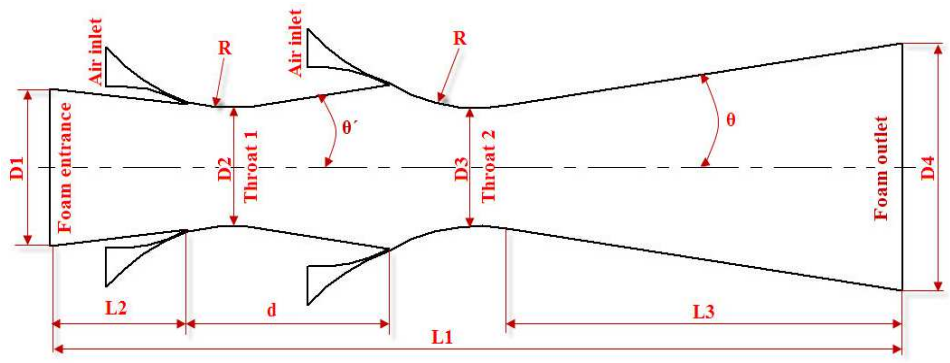

Figure.8. Analytical model of second kind of foam breaker

Figure 9 shows that the value of the negative pressure near the first stage nozzle is smaller than that of the second stage nozzle. As the annular slit distance increases, the value of the negative pressure near the first stage nozzle decreases gradually whereas the pressure valley near the second nozzle remains essentially unchanged. The negative pressure between two nozzles generates an overlapping area when the annular slit distance is smaller. The overall area of the negative pressure between two nozzles almost disappears when the annular slit distance increases to 150 mm. From the point of the general applicability, the best annular slit distance for this type of foam breaker is 50 mm.

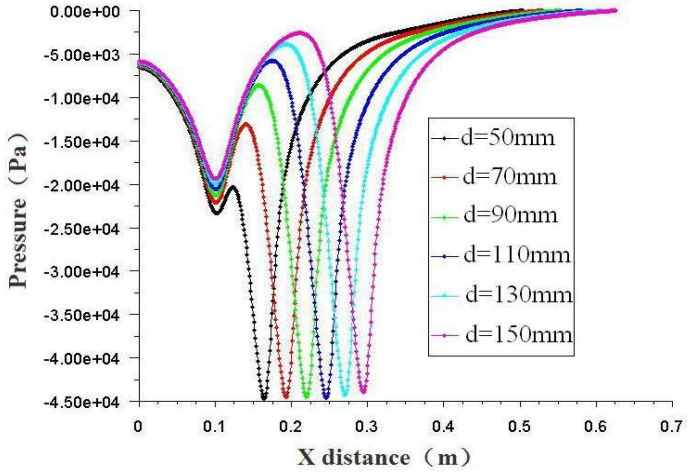

Figure.9. The pressure distribution along the center axis of the foam breaker(y=0)

To increase the overlap area between two nozzles, we designed a third type of analytical model for the two-stage Laval annular foam breaker as shown in Fig. 10. The angle of the first diffuser is 0(θ´=0°), and both throat planes are equal (D2=D3=60 mm).

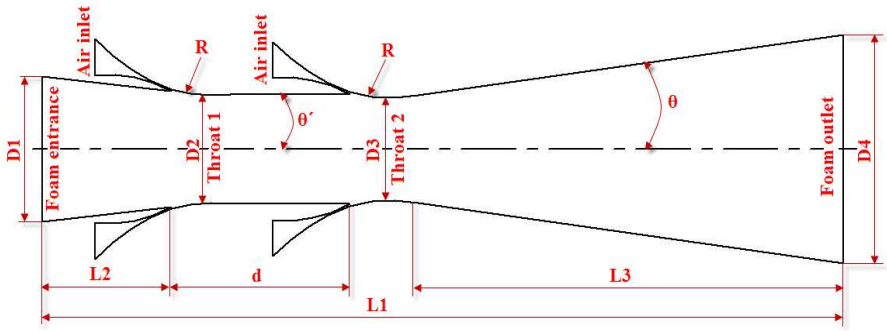

Figure.10. Analytical model of third kind of foam breaker

With the increasing of the annular slit distance, the absolute value of negative pressure near first stage nozzle decreases gradually while the pressure near the second nozzle remains almost unchanged as shown in Figure 11. However, the range of the negative pressure increases as the annular slit distance increases. The larger negative

pressure range is more conducive to foam breaking. Thus, the best annular slit distance of the third type of foam breaker is 150 mm.

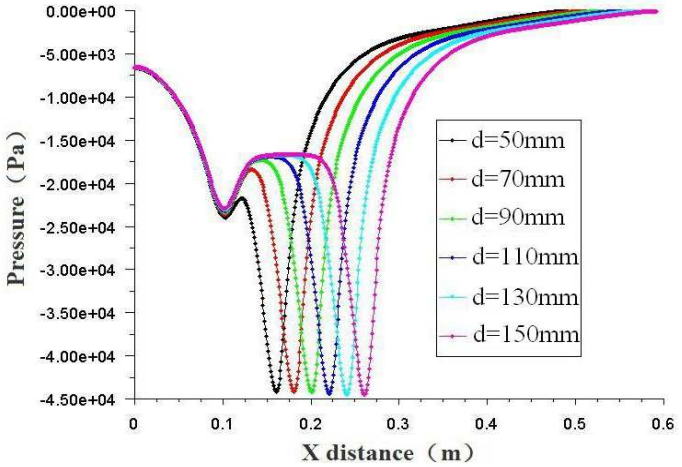

Figure.11. The pressure distribution along the center axis of the foam breaker(y=0)

Figure 12 shows the pressure distribution curves along the center axis of the three types of annular foam breakers. The figure shows that the absolute values of the negative pressure near the nozzle are 30 kpa and 42 kpa, respectively, in the first type of foam breaker, whereas the absolute values are approximately 24kpa and 45kpa for the second and the third type of foam breakers, respectively. The third foam breaker with the annular slit distance of 150 mm has a larger range of negative pressure than those of the others. It is more conducive when foam drilling fluid has a large volume and high flow rates. Considering the overall size and weight factors of the foam breaker, we recommend the annular slit distance to be less than 100 mm for the third type of foam breaker.

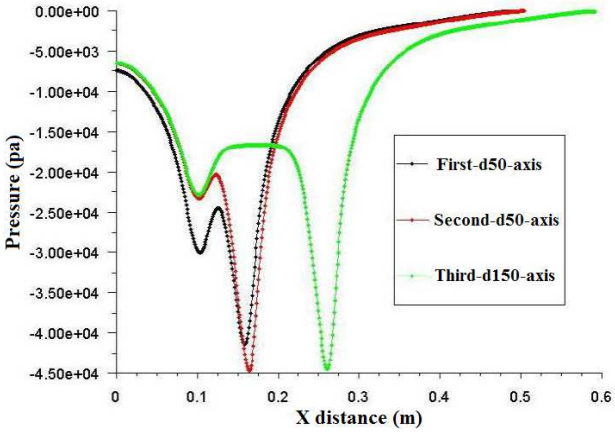

Figure.12. Pressure distribution curves of three forms of foam breaker

CONCLUSION

A novel two-stage Laval annular mechanical foam breaker was designed. The flow characteristics of the annular foam breaker were investigated using CFD simulation. This study has the following conclusions:

(1) Maximum velocity and negative pressure are generated near the second throat plane. The angle of the first diffuser and the annular slit distance have an important influence on the value and distribution of the negative pressure inside the annular foam breaker.
(2) The value of the negative pressure along the axis of the foam breaker can be approximately 45 kPa when the angle of the first diffuser was 0 and the annular slit distance was 150 mm. In addition, the range of the internal negative pressure was larger than others.
(3) Considering the overall size and weight factors of the foam breaker, we recommend the annular slit distance to be less than 100 mm for the third type of foam breaker. However, its actual effect must be verified by further experiments and application in drilling sites.

Acknowledgement
The research presented in this paper was supported by The Scientific Forefront and Interdisciplinary Innovation

Project of Jilin University (No.2013ZY03) and The Key Technologies of Rapid Drilling in Mine Emergency Rescue (No.2013911033).

REFERENCES

[1] L.P. Wan, Y.F. Meng, and Y.J. Li.. *Drilling & Production Technology*, **2010**, **33**(1), 76-79.
[2] W.H. Zhao. *Natural Gas Industry*, **1999**, **19**(5), 51-54.
[3] R.R. Teichrob, and J.J. Manuel. *Oil Gas J*, **1997**, **95**(33), 52-55.
[4] Z. Chen. Study of cuttings transport with foam under elevated pressure and elevated temperature conditions, University of Tulsa, PhD Dissertation, **2005**, 90-96.
[5] P.L. Cao, J.C. Zhang, X. Wu, and J.Y. Huang. *Global Geology*, **2009**, **12**(4), 204-209.
[6] J.S. Song, S.X. Ou, Z.M. Shan, and G.Q. Zhang. *Oil Drilling & Production Technology*, **1998**, **20**(6), 24-28.
[7] A.S. Paknejad. Foam Drilling Simulator. Texas A&M University, **2005**, 1-2.
[8] D.S. Liu，Z.H. Li, and X.L. Liu. *Drilling Fluid & Completion Fluid*, **2006**, **23**(1), 11-14.
[9] S.J. Neethling, H.T. Lee, and J.J. Cilliers. *Minerals Engineering*, **2003**, **16**(11),1123-1130.
[10] Y.X. Wang, J.F. Lu, and F.Q. Xie. *Tianjin Chemical Industry*, **2011**, **25**(4), 37-39.
[11] W.D. Wang, Z.S. Qiu and K.H. Lu. *Oilfield Chemistry*, **2008**, **25(1)**,1-4.
[12] C.Y. Chen, S.C. Baker, and R.C. Darton. *J Chem Technol Biotechnol*. **2006**, **81**,1923–1931,
[13] R. Pelton. *Journal of Industrial Microbiology & Biotechnology*, **2002**, **29**(4), 149-154.
[14] A.G. Vetoshkin.. *Theoretical Foundations of Chemical Engineering*, **2003**, **37**(4), 372-377.
[15] N.M. Guzman, Foam Flow in Gas-Liquid Cylindrical Cyclone Compact Separator, University of Tulsa, **2005**, 59-61.
[16] A.G. Vetoshkin, and B.A. Chagin. *Theoretical Foundations of Chemical Engineering*, **2002**, **36**(2), 113-117.
[17] N.S. Deshpande, and M. Barigou. *J Chem Technol Biotechno*, **1999**, **74**,979-987.
[18] T. Satoshi, O. Masayuki, Y. Masanori, Y. Kazuaki and O. akira. *J Chem Technol Biotechno*, **2003**,**78**(1), 48-55..
[19] S. Takesono, M. Onodera, K. Toda, M. Yoshida, K. Yamagiwa, and A. Ohkawa. *Bioprocess Biosyst Eng*, **2006**, **28**(4): 235-242.
[20] N.V. Zagoskina, and O.M. Sokovnin. *Theoretical Foundations of Chemical Engineering*, **2001**, **35**(1), 95-98.
[21] M. Barigou. *Chemical Engineering and Technology*, **2001**, **24**(6): 659-663.
[22] T. Satoshi, O. Masayuki, Y. Masanori, Y. Kazuaki, and O. Akira. *Journal of Chemical Engineering of Japan*, **2007**, **40**(7), 565-570.
[23] N.S. Deshpande, and M. Barigou. *Chem Eng Process*, **2000**, **39**(3): 207-217.
[24] P.L. Cao, W.Y. Ma, Z.G. Zhang, G.C. Liu, and X.L. Liu. *Petroleum Drilling Techniques*, **2011**, **39**(5)： 49-52.
[25] P.L. Cao, Z.Y. Hu, B.Y. Chen, and Z.C. Zhen. *IJE Transactions B*, **2012**, **25(**1): 73-79.
[26] P.L. Cao, B.Y. Chen, Z.C. Zhen, and W.Y. Ma. *IJE Transactions* C, **2012**, **25**(2): 111-118.
[27] M.H. Qahtan, Y.H. Sun, O. Yarbana, L. Xu and A. Fahmi. *Global Geology*, **2007**, **10**(1): 34-38.